

Experimental Investigation of Efficiency and Deposit Process Temperature During Multi-Layer Friction Surfacing

Zina Kallien^{1,a*}, Arne Roos^{1,b}, and Benjamin Klusemann^{1,2,c}

¹Institute of Materials Mechanics, Solid State Materials Processing, Helmholtz-Zentrum Hereon, Max-Planck-Straße 1, 21502 Geesthacht, Germany.

²Institute of Product and Process Innovation, Leuphana University of Lüneburg, Universitätsallee 1, 21335 Lüneburg, Germany.

^azina.kallien@hereon.de, ^barne.roos@hereon.de, ^cbenjamin.klusemann@hereon.de

Keywords: Multi-Layer Friction Surfacing, Temperature, Solid State Layer Deposition, Additive Manufacturing, Dissimilar Aluminum Alloys

Abstract. Multi-layer friction surfacing (MLFS) follows the principle of the friction surfacing (FS) process, which is an established solid state coating technology for similar and dissimilar metallic materials. With this approach, the deposition of a consumable material on a substrate is enabled via friction and severe plastic deformation (SPD), processing the material below its melting temperature. The focus of the present study lies on the investigation of the temperature distribution during MLFS deposition. The measurements show that the temperature within the stack tends to be slightly higher on the advancing side. Additionally, the deposition behavior, i.e. deposition rate and consumable stud consumption rate, was investigated. Along MLFS stack height, deposition efficiency tends to slightly decrease, shown by decreasing layer thickness and increased length of remaining consumable studs. Overall, MLFS is highly repeatable for multiple layers and presents stable deposition conditions. Additionally, the technique has a comparatively low heat input to the substrate and the already deposited material.

Introduction

The technique of friction surfacing (FS) was first named in a patent by Klopstock and Neelands [1] in 1941. It is a solid state coating technology for various metallic material combinations, e.g. aluminum [2], steel [3], magnesium [4], titanium [5] or even dissimilar combinations like aluminum and steel [6]. A stud as consumable material experiences a rotational speed and an axial force and is pressed onto the substrate surface. Friction occurs and the tip of the stud deforms and plasticizes. A relative translational movement between stud and substrate enables the deposition of plasticized consumable material on the substrate. As a discontinuous process, the dimensions of the layer are restricted by the dimension of the used stud. The three main process parameters, i.e. rotational speed, axial force and travel speed, mostly determine the resulting deposit dimensions, which is extensively discussed in the literature for different material combinations, for more details the interested reader is referred to the review paper by Gandra et al. [7]. Additionally, correlations between process parameters, temperature and the geometric dimensions of the deposit have been identified [8, 9].

The potential of the FS process is beyond being a solid state coating technology. Since it is possible to deposit multiple layers on top of each other, known as multi-layer friction surfacing (MLFS) or friction surfacing layer deposition (FSLD), the procedure has proven feasibility as solid state additive manufacturing (AM) technique [10]. Building a layer-by-layer structure using conventional AM techniques based on material fusion is also feasible for various material combinations [11], however, remaining challenges are often a result of material melting and pronounced thermal gradients within the structure, e.g. porosity formation or heterogeneous microstructure [12] as well as residual stresses [13]. In contrast, the deposits via MLFS typically show a fine grained homogeneous microstructure [14] and a good bonding, where the roughness of the preliminary layer helps the mechanical anchoring [15].

To allow a further development of FS as solid state AM technology, the present study analyzes the temperature evolution during the deposition process not only for single layers, but in particular

for a multi-layer stack. For this purpose, MLFS was performed using dissimilar aluminum alloys as substrate and consumable material. During the deposition, the process temperature was measured in the substrate as well as within the stack after three deposited layers in order to get a fundamental understanding of the temperature and re-heating of the structure due to the subsequent deposits. Additionally, the built stack as well as the remaining studs were analyzed with regard to deposition volume and process efficiency.

Materials and Methods

The FS process is the basis for every MLFS deposit and can be divided into two process phases. First, the plasticizing phase is initiated when a rotational speed and an axial force are applied to the consumable stud that is positioned above the substrate. As a result, the stud is pressed onto the substrate surface and friction occurs at the materials' interface. Heat is generated and the tip of the stud starts to plasticize. Afterwards, the deposition phase is initiated by applying a relative translational movement between stud and substrate, which enables the deposition of plasticized consumable material on the substrate as a layer. The process ends when the desired length is achieved or the stud is consumed and the remaining stud material is retracted.

The experiments of this study were performed using a friction welding equipment that was designed for the purpose of FS (RAS, Henry Loitz Robotik, Germany). The machine provides a working area of 0.5 m × 1.5 m and allows forces up to 60 kN, torques of 200 Nm and rotational speeds of 6000 rpm. Displacements and forces in x-, y- and z-direction as well as torque and rotational speed are recorded during the process. For this investigation, two dissimilar aluminum alloys were chosen, i.e. AA 5083 H112 as consumable material (20 mm diameter, 125 mm length) and AA 7050 T7451 as substrate material (300 mm length, 130 mm width, 10 mm thickness). Between substrate and machine table, an AA 7050 T7451 backing plate (300 mm length, 130 mm width, 8 mm thickness) was used.

Six layers were deposited at constant process parameters, i.e. rotational speed of 1200 rpm, axial force of 8 kN and travel speed of 6 mm/s. The deposition processes were performed force-controlled. Between the layer depositions, the MLFS structure cooled down to room temperature. The final six-layer stack showed approx. 8.7 mm height and 153 mm length, see Fig. 1. A stable process behavior is observed for each deposited layer, similar to the example of the second layer, which is presented in Fig. 2.

In order to measure the process temperature, holes of 1 mm in diameter were drilled from the backside into the substrate until 0.5 mm below the substrate surface, see Fig. 4(a) for the spatial distribution. After three deposited layers, three additional holes were drilled from the backside through the substrate into the MLFS structure ending approx. 0.5 mm below the surface of the third layer in order to measure the temperature in the stack during the deposition of the following layers, see Fig. 4(b). The pre-programmed welding distance is 140 mm and the temperature was measured after half of the welding distance.

In order to analyze the position of the thermocouples with regard to the deposited stack and to investigate the layers' geometry, the stack was cut and the samples were embedded, ground and polished. In addition to the cross sections with the holes taken at half of the stack length, cross sections were taken 55 mm from the beginning and 55 mm from the end along the stack length in order to measure the geometric dimensions of the deposited layers as well as for microstructure analysis and hardness testing. A light optical microscope VHX-6000 (Keyence, Germany) was used to analyze the cross sections taken along the stack length. Furthermore, etching with Barker's solution for 90 s at 25 V allows to analyze the microstructure. In addition, micro-hardness testing was performed according to DIN EN ISO 6508-1 using the automated hardness testing machine Durascan 70 G 5 (EMCO-TEST Prüfmaschinen GmbH, Austria). A Vickers indenter with 136° opening angle was used to apply a load of 0.2 kg. The grid size for the hardness mapping was 0.5 mm.

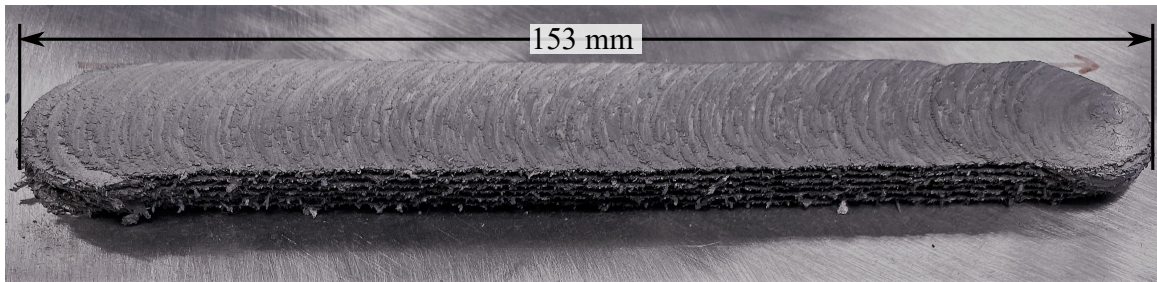


Fig. 1: MLFS stack with six layers deposited at constant process parameters of 1200 rpm rotational speed, 8 kN axial force and 6 mm/s travel speed.

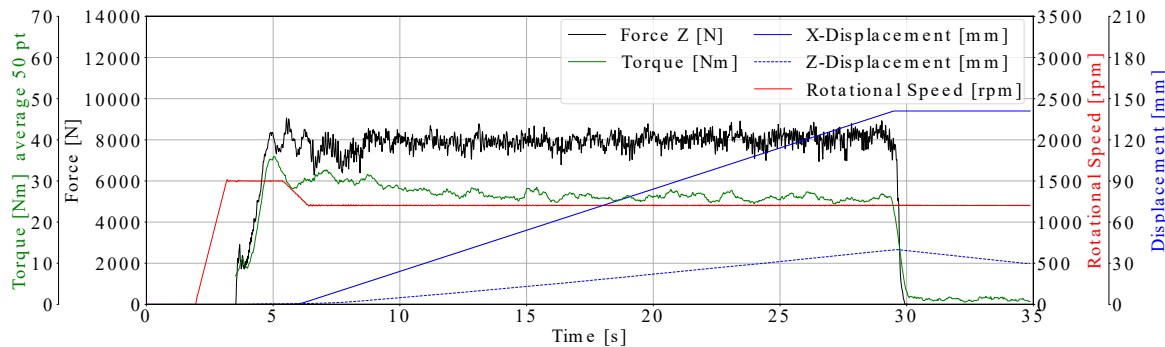


Fig. 2: Process characteristics in terms of torque, force, rotational speed, z- and x-displacement, recorded for the second layer of the six-layer stack. Constant deposition parameters were used for each deposited layer, i.e. 1200 rpm rotational speed, 8 kN axial force and 6 mm/s travel speed.

Results and Discussion

Microstructure and Hardness Analysis. The cross section of the six-layer MLFS stack is shown in Fig. 3(a). For all layer depositions, a repeatable process behavior was observed. The cross sections present the process-characteristic unbonded edges of the layers on the advancing and the retreating side. Similar to findings by Shen et al. [14], the layers show a homogeneous and fine grained microstructure. The etched cross section, extracted 55 mm from the beginning along the stack length, also reveals the area where the substrate material shows a grain refinement, indicating the thermo-mechanically affected zone (TMAZ).

The hardness mapping performed for one sample taken 55 mm from the end along the MLFS stack length shows a homogeneous hardness distribution of the deposited layer material, Fig. 3(b), in the range of AA 5083 H112 base material, which is 91 HV [16]. The hardness distribution clearly illustrates the heat affected zone (HAZ) in the substrate material. The decreased hardness in this area of the substrate can be explained by the recrystallization and precipitation behavior of the alloy [17]. The thermal input during welding can lead to dissolution of precipitates leading to material softening and loss in mechanical properties within the HAZ, as shown for friction stir welding of AA 7075 [18].

Temperature Measurements during MLFS. The temperature measurements performed in the substrate show a maximum process temperature of 393°C during the deposition of the first layer, see Fig. 4(a). The overall process temperatures in the substrate significantly decrease for the deposition of further layers due to the increasing distance. For instance, the deposition of Layer 2 led to a maximum temperature of 339°C, where for the subsequent layer only 301°C was observed. The decrease in maximum process temperature continues for the deposition of further layers, however, gets less pronounced. The sixth layer led to a maximum process temperature in the substrate of 231°C. The decrease in process temperature in the substrate for additional MLFS layers is most significant in the center, see Thermocouple 5 in Fig. 4(a).

The additional process temperature measurements within the stack were performed for the deposition of layers 4-6, see Fig. 4(b). The thermocouples positioned in Layer 3 of the stack recorded a

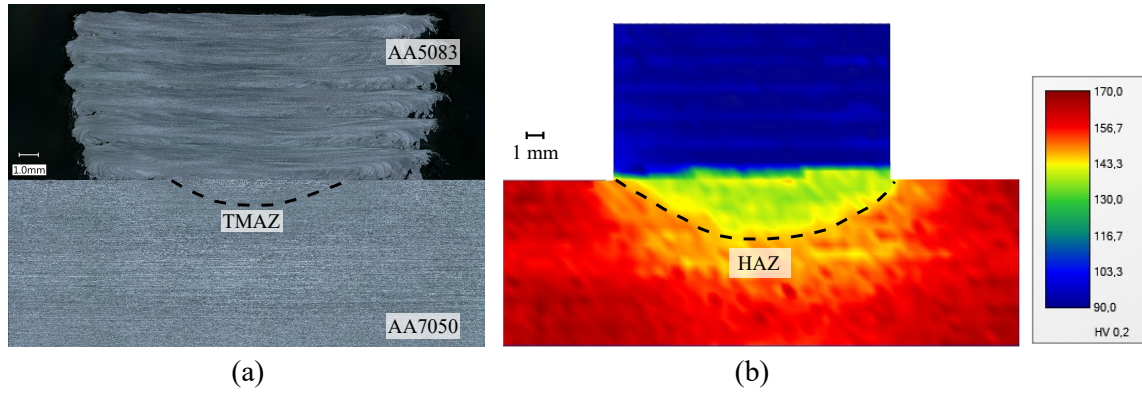


Fig. 3: Cross section as well as etched cross section indicating the thermo-mechanically affected zone (TMAZ) (a) and hardness distribution revealing the heat affected zone (HAZ) (b) of MLFS stack deposited at constant process parameters, i.e. 1200 rpm, 8 kN and 6 mm/s.

maximum temperature up to 372°C during the deposition of Layer 4. Since the distance to the process zone gets larger for every additional layer, the measured maximum temperature in Layer 3 decreased with each additional layer. With the deposition of Layer 6, process temperatures up to 296°C were recorded by the thermocouples within Layer 3. The measurements in the stack showed slightly higher maximum process temperatures on the advancing side than on the retreating side. This observation is in accordance with studies on FS [19, 20] and might be related to the material flow.

The solid state approach of MLFS as AM technology has a significantly lower heat input to the substrate and induces less re-heating of the structure compared to fusion-based AM technologies. For instance, Bock et al.[21] measured the process temperature during laser metal deposition (LMD) of AA 5087. Within the fusion zone, the temperature is obviously above the melting temperature but even 10 mm away from the deposition path a maximum process temperature of approx. 270°C during deposition of the first layer was observed. Similar temperatures during MLFS were recorded by Thermocouple 3 in this study, however, less than one millimeter away from the stack. Although this is a rough comparison, it gives a first impression of the significantly reduced heat input to the substrate in this solid state AM process.

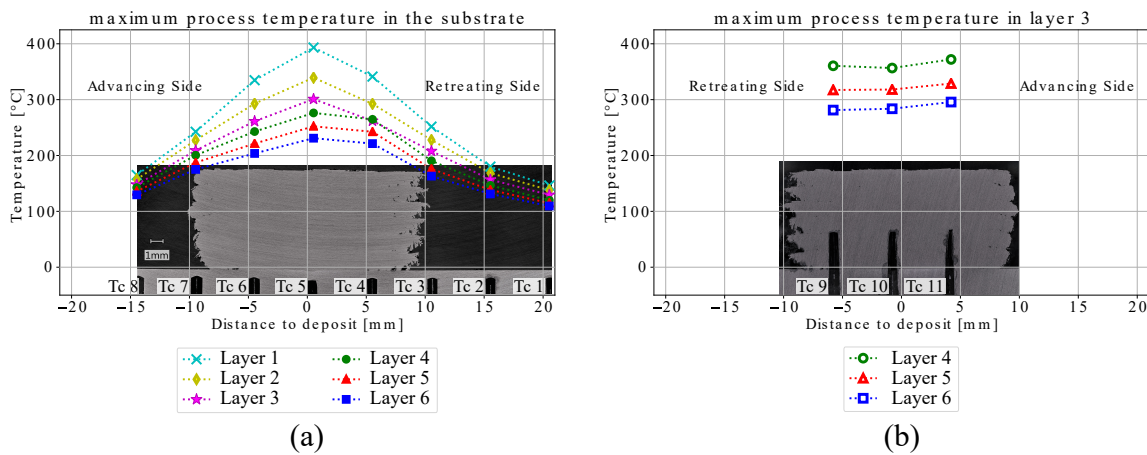


Fig. 4: Maximum process temperature during deposition measured in the substrate (a) and within the third layer of the stack (b).

Deposition rate during MLFS. Although a repeatable and stable process behavior was observed resulting in a homogeneous microstructure and hardness distribution along the stack height, changes in layer thickness are identified for subsequent layers. Along the stack height, the stud consumption is

lower, which is indicated by a decreasing deposit thickness and increasing length of the remaining consumable stud for an increasing number of MLFS layers, see Fig. 5(a). The remaining consumable studs are shown in Fig. 5(c). It can be observed that the increase in remaining stud length and decrease in deposit thickness is more pronounced for the first three layers, where afterwards the deposit thickness and remaining stud length are almost constant. The deposition conditions for the first layers are significantly different since the heat conduction at the beginning of the deposition process is mainly determined by the substrate. For instance, the substrate material has different heat conduction properties as the deposited material, leading to different heat transfer conditions. The more layers are deposited, i.e. the higher the stack, the more equal are the deposition conditions for each subsequent layer, which is shown by similar deposit thicknesses and remaining stud length after the deposition. For the first layer, which is deposited directly on the substrate, the deposition conditions are also differing with regard to friction due to different surface conditions. It has to be considered that every deposited layer leads to a thermo-mechanical impact on the previously deposited structure. However, the present analysis of the stack, i.e. layer geometry, hardness and microstructure, was performed after deposition of all six layers.

Gandra et al.[22] analyzed the performance and efficiency of single layer FS deposition process. For this purpose, the rod consumption rate (CR) is calculated as

$$CR = \pi r^2 V_z \rho, \quad (1)$$

with the mass density for AA 5083 $\rho = 2.66 \text{ g/cm}^3$, r represents the consumable stud radius and V_z the plunge speed of the stud. Similarly, the deposition rate (DR) can be calculated as

$$DR = A_d v \rho, \quad (2)$$

where v denotes the travel speed and A_d the cross section of the deposit. Finally, the deposition efficiency is defined as [22]

$$\eta_{deposition} = \frac{DR}{CR}. \quad (3)$$

The calculated deposition and consumption ratios for the investigated stack as well as the resulting deposition efficiency for the deposited layers are shown in Fig. 5(b). The results show that CR and DR are slightly decreasing for increasing stack height leading to a slightly reduced $\eta_{deposition}$. For the investigated material combination, the results reveal a slightly less efficient deposition with increasing number of deposition layers, however, after a very limited number of layers, the MLFS depositions are uniform, i.e. a constant deposition rate is achieved.

Summary

The MLFS technique was investigated in terms of process temperature within the substrate as well as in the deposited material. Additionally, the deposition rate along the MLFS stack height was analyzed. The results underline the potential of multi-layer friction surfacing as solid state additive manufacturing approach and the main findings can be summarized as follows:

- The measured process temperatures during MLFS are consistently below 400°C for thermocouples 0.5 mm below the substrate surface.
- The measurements within the layer material showed slightly higher maximum process temperatures on the advancing side than on the retreating side.
- The deposition rate tends to be slightly higher for the first layers of the MLFS stack where in particular the first layer shows a thicker deposit and a shorter remaining consumable stud. This behavior can be associated to the different deposition (heat transfer) conditions for the first layers. Subsequently, the heat transfer conditions are more uniform leading to similar deposition rates for the following layers.

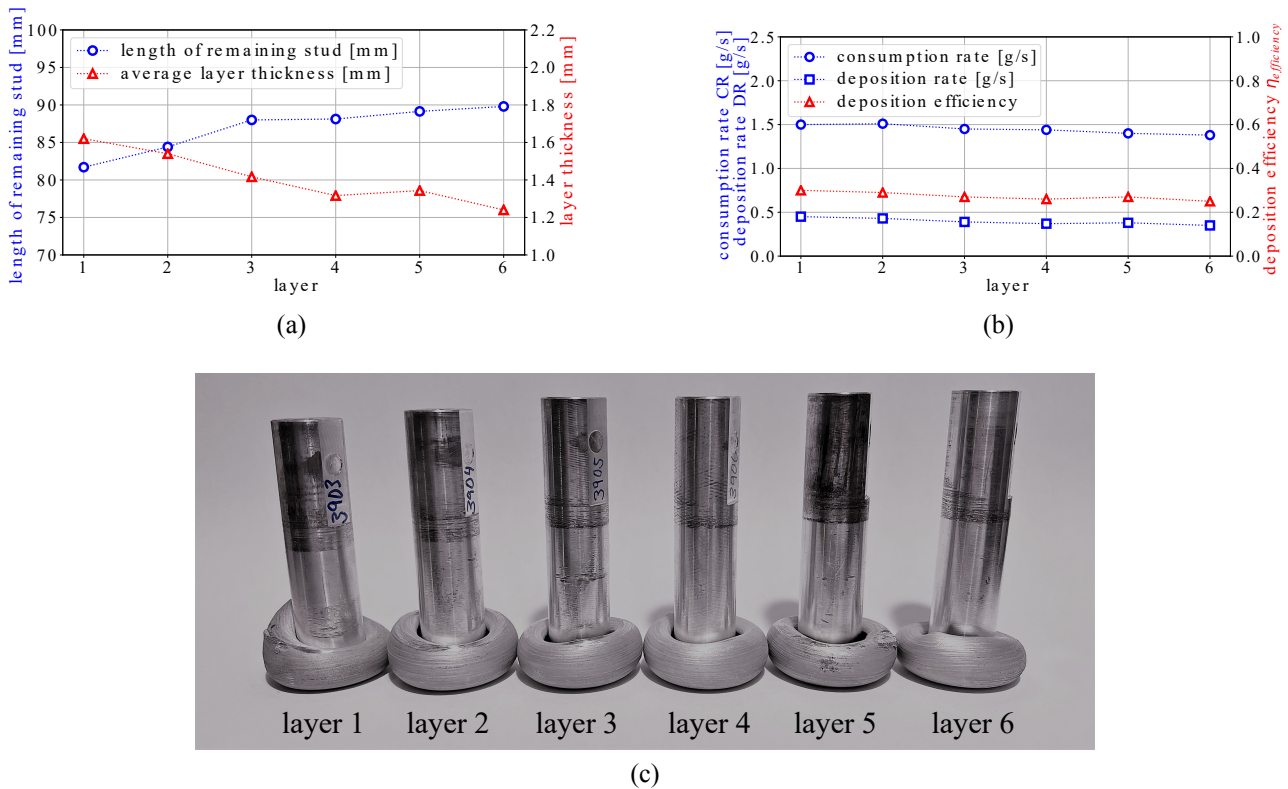


Fig. 5: Deposit layer thickness and remaining stud length (a) as well as consumption rate (CR), deposition rate (DR) and deposition efficiency ($\eta_{deposition}$) according to Gandra et al. [22] for MLFS stack of six layers, which were performed at constant process parameters of 1200 rpm, 8 kN and 6 mm/s; the remaining consumable studs after each layer deposition are shown in (c).

Funding

Benjamin Klusemann acknowledges funding from the European Research Council (ERC) under the European Union's Horizon 2020 research and innovation programme (grant agreement No 101001567).

Data Availability

The obtained data of this research is online available at Zenodo (DOI: 10.5281/zenodo.5902086).

References

- [1] H. Klopstock and A. R. Neelands. An improved method of joining or welding metals, british patent specification 572789, 1941.
- [2] J. Gandra, D. Pereira, R. M. Miranda, and P. Vilaça. Influence of Process Parameters in the Friction Surfacing of AA 6082-T6 over AA 2024-T3. *Procedia CIRP*, 7:341–346, 2013.
- [3] D. Govardhan, K. Sammaiah, K.G.K. Murti, and G. Madhusudhan Reddy. Evaluation of bond quality for stainless steel-carbon steel friction surfaced deposits. *Mater. Today: Proc.*, 2:3511–3519, 2015.
- [4] Dai Nakama, Kazuyoshi Katoh, and Hiroshi Tokisue. Some characteristics of az31/az91 dissimilar magnesium alloy deposit by friction surfacing. *Mater. Trans.*, 49(5):1137–1141, 2008.

-
- [5] V. Fitseva, H. Krohn, S. Hanke, and J. F. Dos Santos. Friction surfacing of Ti-6Al-4V: Process characteristics and deposition behaviour at various rotational speeds. *Surf. Coat. Technol.*, 278:56–63, 2015.
- [6] Hongjun Li, Wei Qin, Alexander Galloway, and Athanasios Toumpis. Friction surfacing of aluminium alloy 5083 on dh36 steel plate. *Metals*, 9(4):479, 2019.
- [7] J. Gandra, H. Krohn, R. M. Miranda, P. Vilaça, L. Quintino, and J. F. Dos Santos. Friction surfacing—a review. *J. Mater. Process. Technol.*, 214(5):1062–1093, 2014.
- [8] F. Y. Isupov, O. Panchenko, L. Zhabrev, I. Mushnikov, E. Rylkov, and A. A. Popovich. Finite Element Simulation of Temperature Field during Friction Surfacing of Al-5Mg Consumable Rod. *Key Eng. Mater.*, 822:737–744, 2019.
- [9] Z. Kallien, L. Rath, A. Roos, and B. Klusemann. Experimentally established correlation of friction surfacing process temperature and deposit geometry. *Surf. Coat. Technol.*, 397:126040, 2020.
- [10] J. J. S. Dilip, S. Babu, S. Varadha Rajan, K. H. Rafi, G. D. Janaki Ram, and B. E. Stucker. Use of friction surfacing for additive manufacturing. *Mater. Manuf. Process.*, 28(2):189–194, 2013.
- [11] D. Herzog, V. Seyda, E. Wycisk, and C. Emmelmann. Additive manufacturing of metals. *Acta Mater.*, 117:371–392, 2016.
- [12] O. Abdulhameed, A. Al-Ahmari, W. Ameen, and S. H. Mian. Additive manufacturing: Challenges, trends, and applications. *Adv. Mech. Eng.*, 11(2):1687814018822880, 2019.
- [13] C Li, ZY Liu, XY Fang, and YB Guo. Residual stress in metal additive manufacturing. *Procedia Cirp*, 71:348–353, 2018.
- [14] J. Shen, S. Hanke, A. Roos, J. F. Dos Santos, and B. Klusemann. Fundamental study on additive manufacturing of aluminium alloys by friction surfacing layer deposition. *AIP Conference Proceedings 2113, 10015 (2019)*, 2019.
- [15] J. C. Galvis, P. H. F. Oliveira, J. de Paula Martins, and A. L. M. de Carvalho. Assessment of process parameters by friction surfacing on the double layer deposition. *Mater. Res.*, 21(3):321, 2018.
- [16] MatWeb - Material Property Data. Aluminum 5083-H112, Accessed 29.11.2021.
- [17] M. Kang and C. Kim. A review of joining processes for high strength 7xxx series aluminum alloys. *J. Weld. Join.*, 35(6):79–88, 2017.
- [18] A. Pastor and H. G. Svoboda. Time-evolution of heat affected zone (HAZ) of friction stir welds of AA7075-T651. *J. Mater. Phys. Chem.*, 1(4), 2013.
- [19] H. Sakihama, H. Tokisue, and K. Katoh. Mechanical properties of friction surfaced 5052 aluminum alloy. *Mater. Trans.*, 44(12):2688–2694, 2003.
- [20] P. Pirhayati and H. Jamshidi Aval. An investigation on thermo-mechanical and microstructural issues in friction surfacing of Al–Cu aluminum alloys. *Mater. Res. Express*, 6(5): , 2019.
- [21] F. E. Bock, J. Herrnring, M. Froend, J. Enz, N. Kashaev, and B. Klusemann. Experimental and numerical thermo-mechanical analysis of wire-based laser metal deposition of Al-Mg alloys. *J. Manuf. Process.*, 64:982–995, 2021.
- [22] J. Gandra, R. M. Miranda, and P. Vilaça. Performance analysis of friction surfacing. *J. Mater. Process. Technol.*, 212(8):1676–1686, 2012.